POLİTEKNİK DERGİSİ

JOURNAL of POLYTECHNIC

ISSN: 1302-0900 (PRINT), ISSN: 2147-9429 (ONLINE)
URL: http://dergipark.org.tr/politeknik

Optimizing A5356 alloy performance with WAAM: a comprehensive study

WAAM ile A5356 alaşım performansının optimize edilmesi: kapsamlı bir çalışma

***Yazar(lar) (Author(s))**: Berfin GURSU[1], Merve Sude KAYIS[2], Hakan ATES[3], Murat KAYAALP[4], Ozge Ece KARA[5]*

ORCID[1]: 0009-0005-7894-8672

ORCID[2]: 0009-0007-0919-1260

ORCID[3]: 0000-0002-5132-4107

ORCID[4]: 0009-0001-3655-1619

ORCID[5]: 0000-0001-5072-6385

To cite to this article: Gursu B., Kayıs M. S., Ates H., Kayaalp M., and Karaca O. E. "Optimizing A5356 Alloy Performance with WAAM: A Comprehensive Study", ***Journal of Polytechnic***, 29(4):290420:1-11 (2026).

Bu makaleye şu şekilde atıfta bulunabilirsiniz: Gursu B., Kayıs M. S., Ates H., Kayaalp M. ve Karaca O. E." Optimizing A5356 Alloy Performance with WAAM: A Comprehensive Study", ***Politeknik Dergisi***, 29(4):290420:1-11 (2026).

Erişim linki (To link to this article): http://dergipark.org.tr/politeknik/archive

DOI: 10.2339/politeknik.1634054

Optimizing A5356 Alloy Performance with WAAM: A Comprehensive Study

Highlights

- *Comparison of porosities over density with Archimedes Principle.*
- *The effect of heat input on the material.*

Graphical Abstract

It was observed that the densities of the samples taken from the production side were higher.

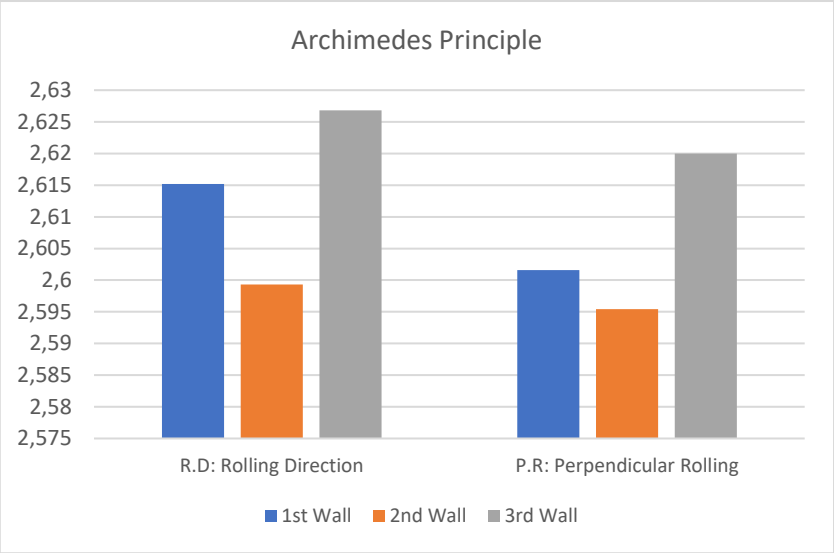

Şekil. Arşimet Prensibine göre yoğunluk hesabı / **Figure.** Density calculation by Archimedes Principle

Aim

This study aims to optimize the performance of A5356 alloy with WAAM with varying heat inputs.

Design & Methodology

The research involves the production of A5356 alloy walls with WAAM at three different heat inputs, followed by mechanical, microstructural, structural characterization and non-destructive evaluations.

Originality

This study contributes to the optimization of additive manufacturing processes of A5356 with heat input variations in WAAM.

Findings

Lower heat input enhanced flexural strength and microhardness; tensile strength was higher parallel to production, with no major defects observed in NDT.

Conclusion

WAAM using optimized heat input parameters offers a promising method for producing A5356 alloy with enhanced mechanical properties and structural integrity, particularly for industrial applications.

Declaration of Ethical Standards

The author(s) of this article declare that the materials and methods used in this study do not require ethical committee permission and/or legal-special permission.

Optimizing A5356 Alloy Performance with WAAM: A Comprehensive Study

(This study was presented at ECRES 2017 conference. / Bu çalışma ECRES 2017 konferansında sunulmuştur.)

Araştırma Makalesi / Research Article

Berfin GURSU[1*], Merve Sude KAYIS[1], Hakan ATES[1], Murat KAYAALP[2], Ozge Ece KARA[3]

[1]Faculty of Technology, Department of Metallurgical and Materials Engineering, Gazi University, Ankara, Turkiye
[2]Gazi University, Graduate School of Natural and Applıed Scıences
Division of Metallurgical and Materials Science Engineering, 06560, Ankara, Turkiye
[3]Intecro Robotics, Yeni Batı 2400. Street, No:13, 06370, Yenimahalle/Ankara, Turkiye
(Geliş/Received : 06.02.2025 ; Kabul/Accepted : 20.08.2025 ; Erken Görünüm/Early View : 12.10.2025)

ABSTRACT

Wire Arc Additive Manufacturing (WAAM) technology is an attractive fabrication method for structural components due to significantly lower consumable usage and higher filler material addition rates than conventional fusion welding. The present study used 1.2 mm welding wire, WAAM CMT-MIG technique, three different wire feed speeds (WFS), and corresponding heat input levels to produce high layer thicknesses. Samples extracted from the fabricated walls were subjected to non-destructive testing methods, including visual inspection (VT), penetrant testing (PT), and ultrasonic testing (UT), as well as various mechanical and material characterization tests such as tensile, flexure, and notch impact tests, microhardness measurements, XRD analysis, and microstructural evaluations using optical microscopy, SEM, and EDS. The results revealed that bending strength and microhardness improved under low heat input conditions. Moreover, these findings indicate that the WAAM technique holds promise as a manufacturing method for A5356 samples when lower heat input is applied.

Keywords: Characterization, WAAM, MIG-CMT, Heat input, A5356 alloy.

WAAM ile A5356 Alaşım Performansının Optimize Edilmesi: Kapsamlı Bir Çalışma

ÖZ

Tel Ark Eklemeli Üretim (WAAM) teknolojisi, geleneksel eritme kaynağına kıyasla önemli ölçüde daha düşük sarf kullanımı ve daha yüksek biriktirme oranları nedeniyle yapısal bileşenler için cazip bir üretim yöntemidir. Bu çalışmada, 1,2 mm kaynak teli, WAAM CMT-MIG (Soğuk Metal Transferi - Metal Soy Gaz) yöntemi kullanılarak üç farklı tel besleme hızı (WFS) ve üç farklı ısı girdisi değeri ile yüksek katman kalınlıklarında üretimler yapılmıştır. Üretilen duvarlardan elde edilen numuneler üzerinde görsel muayene (VT), penetrant testi (PT) ve ultrasonik muayene (UT) gibi tahribatsız muayene yöntemleri ve çekme testi, eğme testi, çentik darbe testi, mikrosertlik, XRD, mikroyapı analizleri (optik mikroskop, SEM ve EDS) dahil olmak üzere çeşitli testler gerçekleştirilmiştir. Sonuçlar analiz edilmiş ve düşük ısı girdisinde eğilme mukavemeti ve mikrosertliğin arttığı ortaya çıkmıştır. Ayrıca, bu sonuçlar WAAM yönteminin daha düşük ısı girdisi ile A5356 numuneler için bir üretim yöntemi olarak umut vaat ettiğini göstermektedir.

Anahtar Kelimeler: Karakterizasyon, WAAM, MIG-CMT, Isı girdisi, A5356 alaşım.

1. INTRODUCTION

Initially referred to as rapid prototyping, Additive Manufacturing (AM) technology emerged in the 1970s, enabling the production of specialized, complex-shaped components that were challenging to fabricate through conventional manufacturing techniques [1–6].

Wire Arc Additive Manufacturing (WAAM) has revolutionized aluminum alloy production by combining high deposition rates (1-4 kg/hour) with material efficiency (30-50% reduction in waste compared to traditional methods) [7, 8].

Recent studies highlight the following:

• The critical role of heat input in microstructure control [9].

• The superior strength-to-weight ratio of A5356 at low heat inputs [10].

This study systematically evaluates three heat inputs (97.17, 125.95, 165.60 J/mm) to optimize WAAM-processed A5356 for industrial applications.

Several studies have explored WAAM as a type of direct energy deposition (DED) process, highlighting its effectiveness in producing complex geometries while minimizing material waste [11-13].

Research has shown that the mechanical properties of components processed using WAAM are strongly influenced by heat input, making process optimization critically crucial for industrial applications [13, 14]. For Al-5356 alloy in particular, optimizing process

*Sorumlu Yazar (Corresponding Author)
e-posta : berfingrs20@gmail.com

parameters is essential for enhancing material reliability and performance [1-18].

Studies have shown that a controlled arc power source is essential for effectively depositing aluminum alloys in WAAM. Moreover, applying low heat input during the Cold Metal Transfer (CMT) process enhances the mechanical properties of WAAM-produced Al-Mg alloys compared to wrought counterparts. This improvement is attributed to reduced porosity and finer microstructures, increasing hardness and tensile strength [18-20, 21-23].

In addition, welding parameters like wire feed rate and travel speed play a crucial role in determining the geometric characteristics of WAAM-produced components [10, 24]. A comprehensive analysis of wire feed speeds, heat input values, and non-destructive testing methods has provided valuable insights for optimizing WAAM in industrial applications [24-28].

Based on the literature review, this study investigates the effects of different heat inputs on across a wide test range, demonstrating the impact of low heat input on material properties [29].

2. MATERIALS AND METHODS

2.1. Materials

Al-5356 aluminum alloy was utilized for welding purposes. The mechanical characteristics of the A5356 (ER5356) welding wire (Ø1.2 mm) are presented in Table 1, and its chemical composition is detailed in Table 2.

Table 1. Mechanical properties of Al-5356 Alloy [30]

Mechanical Properties	Tensile Strength (MPa)	Yield Strength (MPa)	Elongation (%)
Al-5356	260	180	20

Table 2. Chemical composition of ER5356 wire [30]

AWS Code	Chemical Composition (%)			
	Si	**Fe**	**Mn**	**Mg**
ER5356	<0.25	<0.40	0.30	5.00

2.2. WAAM System

The robotic welding system included a *Metal Worm* arm from ABB and a welding machine with a CMT unit from Fronius, as illustrated in Fig. 1. The system consists of a six-axis robot and a two-axis device.

The robotic welding system consisted of:

- ABB MetalWorm 6-axis robotic arm
- Fronius CMT-MIG power source
- 100% Ar shielding gas

Figure 1. Production of the A5356 first wall by the WAAM welding machine [Interco robotic, icmatse2024]

2.3. Production Parameters

Using the MIG-CMT technique and 100% argon as the shielding gas (as shown in Table 3), the wire feed rate (WFS) was set to 4.5 m/min for the first wall, 6 m/min for the second wall, and 8 m/min for the third wall. The walls were produced.

Different heat input levels were achieved by adjusting the welding settings to evaluate the influence of welding parameters on the material's structure and properties. The 1st and 3rd walls exhibited the lowest and highest heat inputs, respectively. To achieve proper bonding, the initial three layers of the first wall were deposited at a wire feed rate of 8 m/min, followed by 6 m/min for the subsequent three layers. Likewise, the first three layers of the second wall were also deposited at a WFS of 8 m/min.

The dimensions of each wall were 200 × 200 mm, consisting of 100 layers with a 2.05 mm interlayer distance. At least three specimens were prepared for each test: tensile, bending, microhardness, microstructure analysis, and XRD analysis.

Additionally, to ensure proper bonding between the substrate and the walls, the preliminary three layers of the first wall were deposited at 8 m/min, followed by 6 m/min for the subsequent three layers. Similarly, the primary three layers of the 2nd wall were also applied at 8 m/min.

The walls were manufactured with a height and length of 200 mm, comprising 100 layers with an interlayer spacing of 2.05 mm. The welding parameters and corresponding heat input variations are comprehensively presented in Table 3. For mechanical and microstructural characterization, a minimum of three distinct conditions are also documented in Table 3.

Table 3. Welding parameters applied during the production of wall structures [icmatse2024]

Walls	WFS (m/min)	Voltage (V)	Current (A)	Heat Input (J/mm)	Layers
1st Wall	4.5	11.8	61	97.17	100
2nd Wall	6	12.8	82	125.95	100
3rd Wall	8	13.8	100	165.6	100

2.4. Testing Protocol

The standards of the tests conducted on the material, the equipment utilized, and the number of specimens extracted are summarized in Table 4. As indicated in the Table, three specimens were aligned parallel to the build direction, while another three spans were oriented perpendicularly. Figure 2 illustrates the specific locations on the wall from which the specimens were obtained. For this configuration, Equation 1 was employed to calculate the heat input.

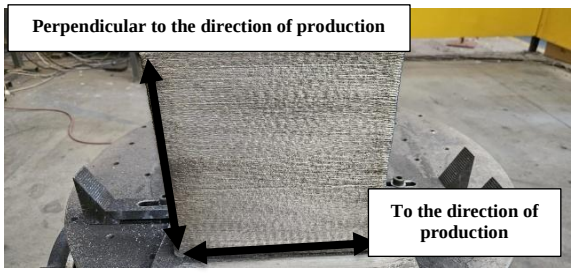

Figure 2. Image of the WAAM wall with sample locations [Interco robotic, icmatse2024]

Heat Input Calculation:

For this setup, the equation was adopted to calculate the heat input.

$$\text{Heat Input (kJ/mm)} = \frac{\eta * V(V) * I(A)}{1000\left(\frac{J}{kJ}\right) * S(mm/s)}$$

Where: η=0.85 (efficiency), V=voltage (V), I=current (A), S=travel speed (mm/s) [28].

2.5. Microstructure Analysis

a. Optical microscope

Optical images of the characterized molded samples were taken at 5x (Fig. 3), 10x (Fig.4), and 20x (Fig. 5-7) magnification. The pores of the material, microstructures, and grain boundaries were observed in the images.

When the optical images (Figs. 3 -7) were analyzed together with SEM images (Figs. 8 and 9), it was observed that the 1st wall had the lowest and the 3rd wall had the highest density in terms of the existence of porosity and the density of Al_2Mg_3 in the material.

When optical images (Figures 3-7) were analyzed together with SEM images (Figures 8, 9), it was observed that the first wall had the lowest porosity and Al_2Mg_3 density. In contrast, the third wall had the highest density. Considering the heat inputs in Table 3, it was observed that the grains grew larger as the heat input increased (Figure 5b > Figure 6b > Figure 7b) and the grain boundaries decreased. In particular, in Figures 3c, 4c, and 7, we observe that the grain size of the third wall increases with high heat input. This leads to a decrease in hardness and, consequently, low strength. In the peaks obtained from XRD analysis, the Al_2Mg_3 compound was observed in the microstructure (Figure 7a and Figure 7c) [31, 32].

Table 4. Standards used to test the material, equipment used, and the number of samples taken [icmatse2024]

Test	Standard	Equipment	Specimens
Tensile	ASTM E8	Instron 5982	3 parallel & 3 perpendicular
Bending	AWS D1.2	5-ton load frame	3
Microhardness	ASTM E384	Wilson VH1150	3
Microstructure	-	OM/SEM	3
XRD	ISO 17405	Bruker D8 Advance	3

a. b. c.

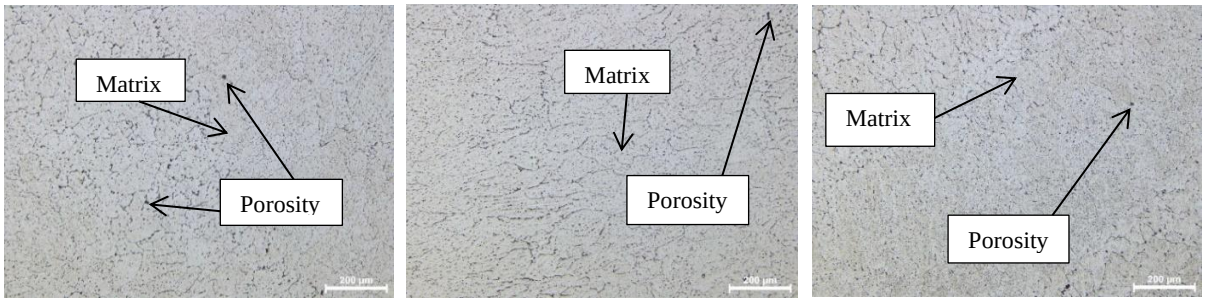

Figure 3. Optical microscope image of the sample of the 1st, 2nd, and 3rd wall at 5x magnification

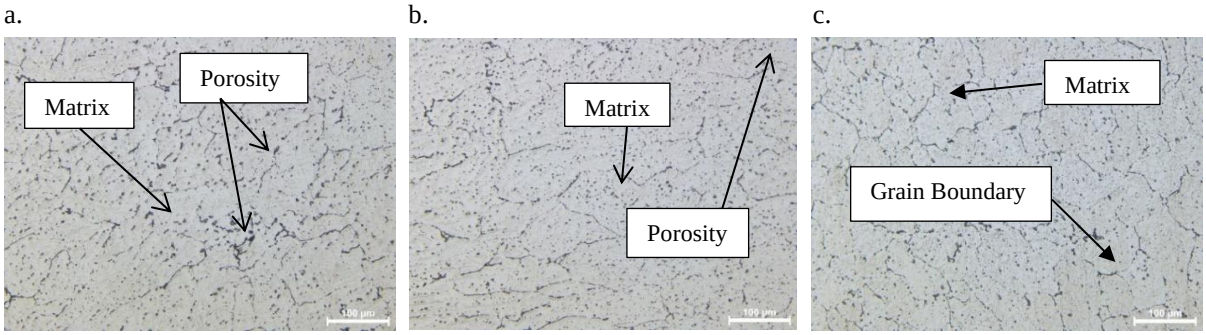

Figure 4. Optical microscope image of the sample of the 1st, 2nd, and 3rd wall at 10x magnification

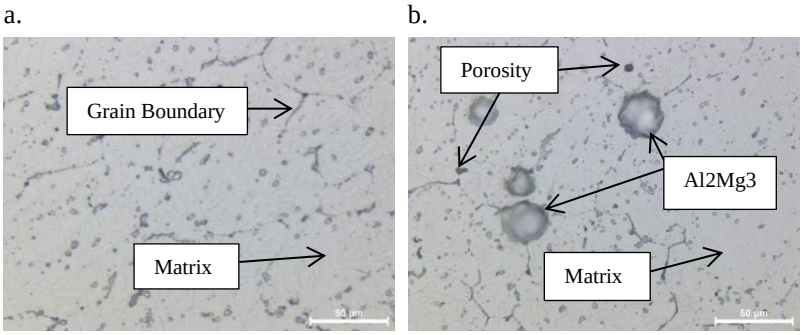

Figure 5. Optical microscope image of the sample of the 1st wall at 20x magnification

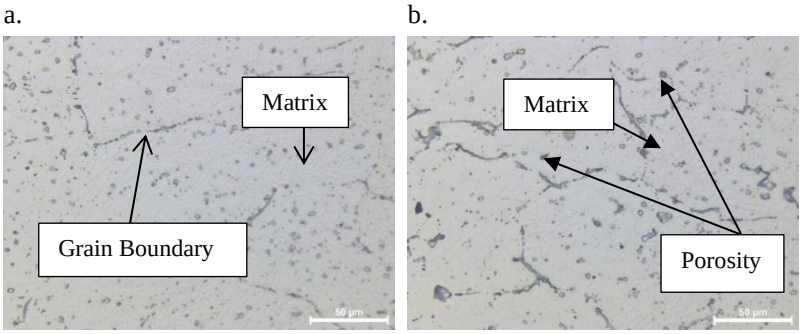

Figure 6. Optical microscope image of the sample of the 2nd wall at 20x magnification

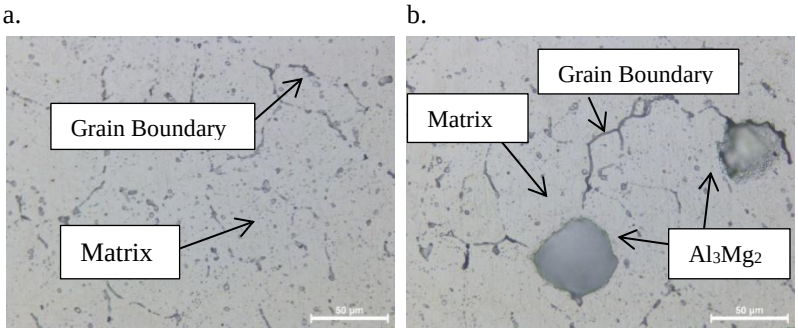

Figure 7. Optical microscope image of the sample of the 3rd wall at 20x magnification

b. SEM analysis

Scanning Electron Microscopy (SEM) is a high-resolution technique to examine materials' surface structure, morphology, porosity, and microstructural characteristics. It also effectively detects defects or variations in microstructure that may occur during production [33].

In WAAM processes, heat input directly affects the microstructure. Low heat input (e.g., Fig. 8a and Fig. 9a) results in a faster cooling rate, promoting fine-grained microstructures, reduced pore formation, and a more homogeneous internal structure. These features contribute to improved mechanical properties. SEM images of such samples show delicate dendritic structures and smooth surfaces.

Conversely, high heat input (e.g., Fig. 8c and Fig. 9c) slows the cooling rate, resulting in coarser grains, visible pores, temperature-induced cracks, and heterogeneity in the microstructure. Expansion of dendritic structures and increased surface porosity are also evident in these cases.

It has been reported that low heat input reduces the grain size and the microstructure becomes more homogeneous [34, 35]. Moderate heat input (e.g., Fig. 8b and Fig. 9b) yields a microstructure between the extremes, potentially balancing mechanical performance and structural uniformity during manufacturing.

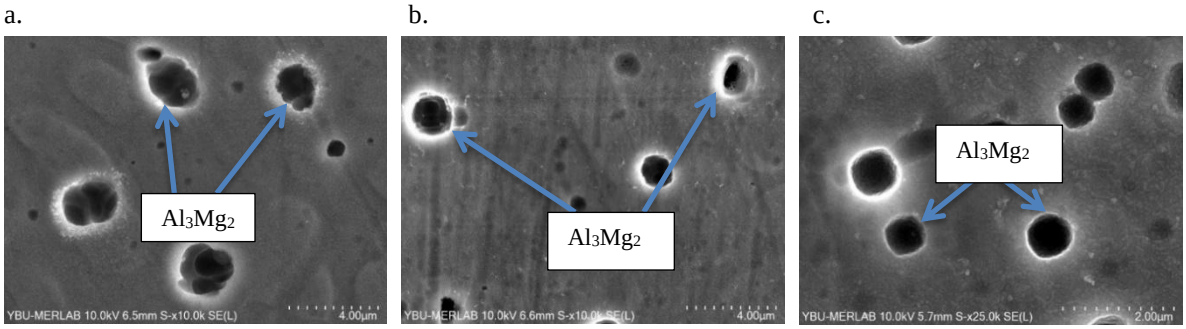

Figure 8. SEM image of wall 1st, 2nd, and 3rd at x10.

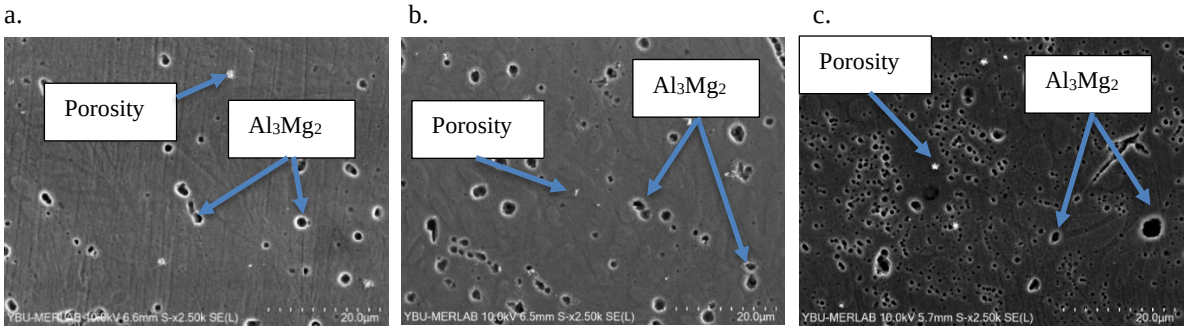

Figure 9. SEM image of wall 1st, 2nd, and 3rd at x2.5.

According to Archimedes' Principle, density measurements revealed that samples taken perpendicular to the rolling direction exhibited lower densities compared to those aligned with the rolling direction. Furthermore, the second wall oriented perpendicular to the rolling direction demonstrated the most favorable heat input and porosity characteristics. Previous studies [36] have indicated that reduced heat input can enhance the microstructure and decrease the porosity of aluminum alloy components.

Although the 1st wall produced has the lowest heat input (97.17 J/mm), density, average tensile strength perpendicular to the production direction, microhardness, SEM-EDS analysis results, and Archimedes' Principle revealed that the 2nd wall should be selected as the optimum material. We also found the phenomenon by examining optical and SEM analysis images. In the 2nd wall with a wire feeding speed of 6 m/min, sufficient time was given for the material $(1+x)^n = 1 + \frac{nx}{1!} + \frac{n(n-1)x^2}{2!} + \cdots$ melt, also the porosities in the microstructure were formed at the optimum level, which caused the second material to give optimum results in the analysis and results.

c. EDS analysis

Energy-dispersive spectroscopy (EDS) was performed to evaluate the chemical composition, identify surface elements, and examine their distribution in Al 5356 specimens produced via the WAAM technique.

Since Al 5356 primarily consists of aluminum, magnesium, and trace alloying elements, EDS provided critical insights into elemental homogeneity, potential impurities, and compositional deviations arising during production.

In WAAM, maintaining a uniform chemical composition is essential, as it directly affects mechanical performance. EDS allowed for qualitative and quantitative analysis of alloying elements and surface phenomena such as oxidation and corrosion. The results confirmed aluminum as the primary component (94.5–94.6 wt%), with magnesium being the second most abundant (4.62–4.78 wt%). Minor elements such as titanium exhibited slight variations depending on heat input. For instance, titanium content decreased from 0.41 wt% in the lowest heat input condition to 0.28 wt% in the highest (Table 5). The relatively higher titanium and manganese levels in the low heat input samples suggest a reduction in oxidation or diffusion effects, consistent with previous findings that associate low heat inputs with enhanced alloy integrity [33].

Additionally, the uniform distribution of aluminum across all samples demonstrated WAAM's capacity to

maintain compositional consistency despite thermal variations. These observations highlight the effectiveness of EDS in linking process parameters with microstructural evolution, contributing valuable feedback for process optimization [33].

Table 5. EDS Analysis

Element	1st Wall Wt%	2nd wall Wt%	3rd Wall Wt%	Standard Name	Factory Standard
Mg	4.64	4.62	4.78	MgO	Yes
Al	94.60	94.57	94.46	Al2O3	Yes
Si	0.09	0.08	0.09	SiO2	Yes
Ti	0.41	0.34	0.28	Ti	Yes
Cr	0.07	0.14	0.07	Cr	Yes
Mn	0.09	0.13	0.16	Mn	Yes
Fe	0.05	0.11	0.10	Fe	Yes
Cu	0.05	0.01	0.05	Pure Element	Yes
Total	100.00	100.00	100.00		

2.6. Structural (XRD) analysis

X-Ray Diffraction (XRD) analysis was performed on a Bruker D8 Advanced instrument. In addition, monochromatic Cu K Kα radiation (λ=1.54056 Å) was used at 40kV and 40 mA operating conditions 10°- 90° angle range, and scanning speed of 0.04 degrees/min.

The experimental results demonstrated that the three specimens produced using an identical welding wire exhibited consistent and comparable physical characteristics. As presented in Figure 10, the joint analysis reveals the orientations of the crystal lattice structures and the corresponding density measurements, providing insight into the material's internal configuration.

The diffraction analysis identified distinct material peaks occurring at specific angles: 38.3239° for the first peak, 44.6357° for the second, 64.7937° for the third, 77.7328° for the fourth, and 81.8551° for the final peak. The XRD peaks of the ER5356 filler wire, whose chemical composition is given in Table 2, and the elemental composition of the produced walls, whose EDS analysis is presented in Table 5, showed that the A5356 alloy primarily comprises the aluminum phase. Other elements, such as magnesium, are integrated into this structure.

Moreover, the width and intensity of these peaks provided information on the material's crystal size and internal stresses. The obtained peaks were the corresponding planes of the aluminum face-centered-cubic crystal structure, respectively [37-39].

In the microstructure of ER 5183 alloy produced by the WAAM-CMT method, the crystallite size and lattice parameters of α-Al and Al_3Mg_2 phases are consistent.

XRD analysis in Figure 10 shows that the (111) point is FCC α-Al, the (200) point is FCC α-Al, the (220) point is Al3Mg2, the (333) point is FCC α-Al, and the (222) point is FCC α-Al [31]. With the values in literature. This information is essential for understanding the microstructure formed in the WAAM process and optimizing the mechanical properties [31].

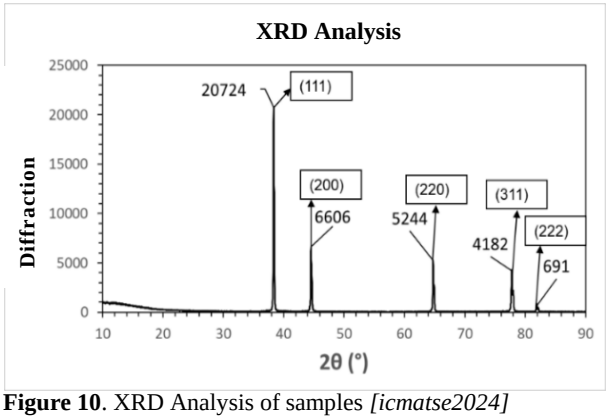

Figure 10. XRD Analysis of samples *[icmatse2024]*

2.7. Tensile Test

The average tensile strength of the A5356 samples produced via the WAAM method was measured at 214 MPa. Variations in tensile strength were observed depending on the orientation of the weld seam; notably, specimens oriented vertically exhibited lower tensile strength compared to those positioned horizontally.

Based on the data presented in Table 6 and Graphs 1 and 2, the average tensile strengths were determined to be 184.53 MPa in the direction perpendicular to fabrication and 270.97 MPa in the direction parallel to fabrication. These findings indicate that the A5356 material produced via the WAAM method can exhibit high mechanical strength under specific conditions. However, given the directional dependence of tensile strength relative to the weld orientation, it is crucial to assess the specimens accordingly.

Images of the tensile test specimens are given in Figure 11.

Figure 11. The specimens after the tensile test

Table 6. Tensile Strength Values Parallel and Perpendicular to the Fabrication Direction

Walls	**Average Tensile Strength (parallel to fabrication direction) (MPa)**	**Average Tensile Strength (Perpendicular to fabrication direction) (MPa)**
1st Wall	270.97	184.53
2nd Wall	263.00	191.84
3rd Wall	272.87	219.20

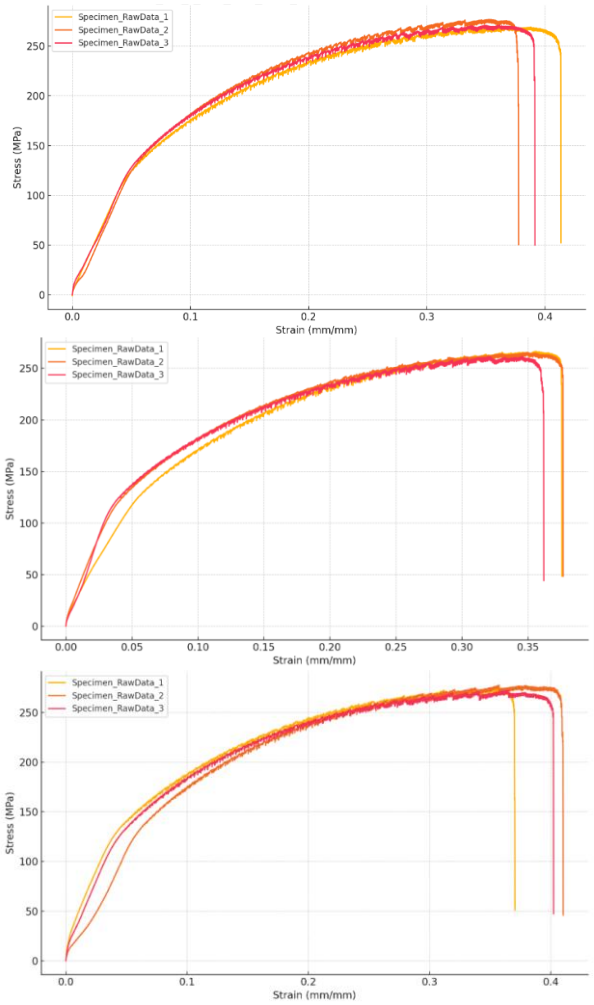

Graphic 1. Tensile strength values perpendicular to the fabrication direction graphics

2.8. Flexure Test

Following flexural test standards, the distance between the supports was set to 80 mm. The flexural test specimens are depicted in Figure 12. During the bending test, the upper supports were lowered at a 3 mm/min rate under a load of 5 tons. The slope graph is presented in Figure 3. Bending stress was found to vary depending on the condition of the specimen, and the graph indicates that walls 1 and 2 exhibited high bending strength.

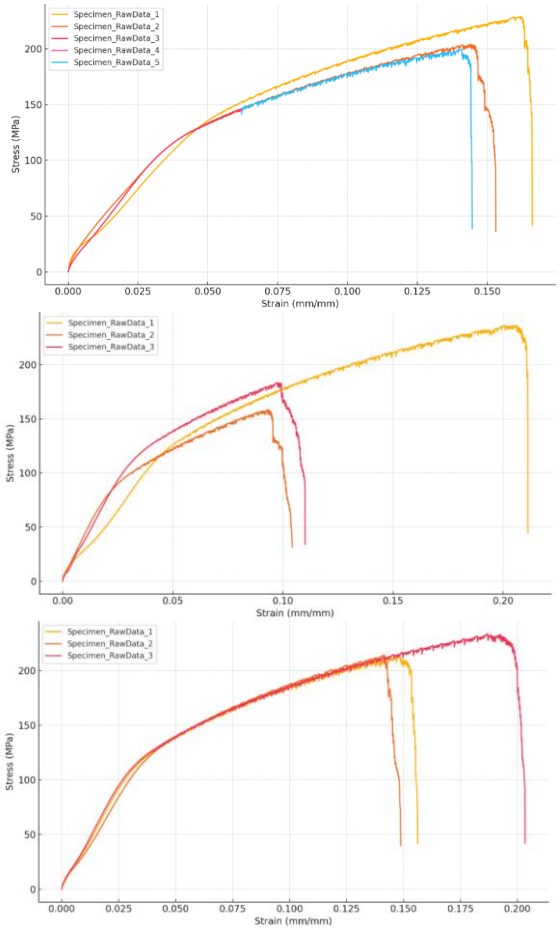

Graphic 2. Tensile strength values parallel to the fabrication direction graphics

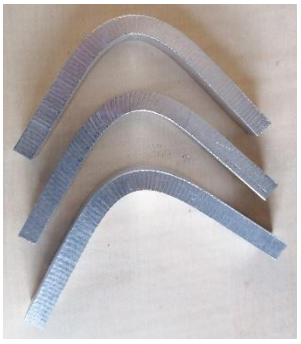

Figure 12. Flexure test specimens

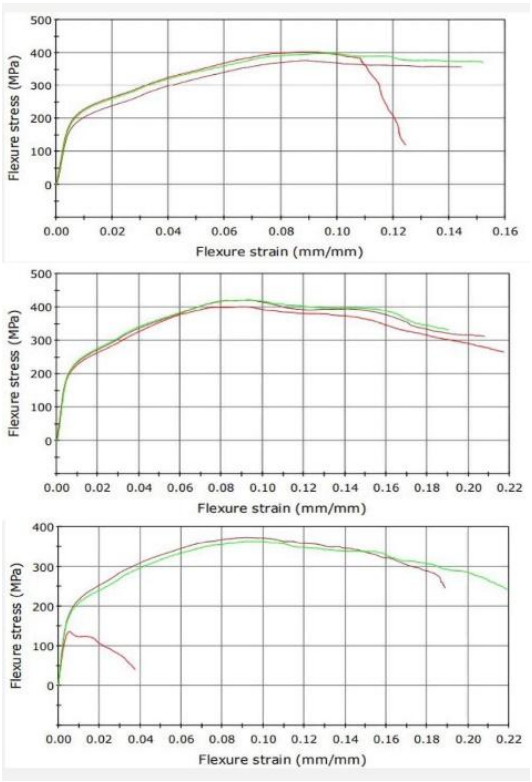

Graphic 3. Flexural Stress–Strain Curves for Walls 1, 2, and 3, respectively

2.9. Hardness Test

Microhardness test results were obtained by applying a 500-gram pyramid-shaped indenter to Bakelite specimens for 10 seconds on pre-sanded and polished surfaces, by HV 0.5 standards. Hardness values were determined by taking three separate measurements from different regions of each specimen, as presented in Table 7. The observed variations in hardness across various areas of the specimens suggest a non-uniform surface hardness, likely resulting from inconsistencies in the material's manufacturing process. Based on the data in Table 7, the first wall's microhardness was higher than that of the others. Supporting literature indicates that increased heat input in Al-Zn-Mg alloys leads to porosity and grain growth, adversely affecting mechanical properties [35].

Table 7. Microhardness measurement results.

Measurement	1st Wall	2nd Wall	3rd Wall
1.	73 HV	70 HV	66 HV
2.	68 HV	72 HV	71 HV
3.	73 HV	71 HV	68 HV
Average	71.33 HV	71 HV	68.33 HV

2.10. Non-Destructive Testing

Visual Testing (VT), Penetrant Testing (PT), and Ultrasonic Testing (UT) were conducted in accordance with relevant standards to identify potential defects in the weld zones produced using the MIG-CMT technique with supplementary A5356 filler wire.

a. Visual test (VT)

In Fig. 13, we thoroughly examined the transitions between the layers and all surfaces with the use of a visual test, AWS D1.2/D1.2M:2014, as depicted in Fig. 13. It was disclosed that there were no cracks, notches, or discontinuities exceeding the acceptance criteria on the material surface.

Figure 13. Specimens subjected to visual inspection [icmatse2024]

b. Penetrant test (PT)

Given the non-magnetic nature of the materials, liquid penetrant testing was performed on the specimens in accordance with EN ISO 3452-1.

As shown in Figure 14, the developer was applied to both surfaces of the specimens and allowed to dwell for 10 minutes, followed by the application of the red penetrant (Figure 15) with a dwell time of 5 minutes. The inspection results indicated that no defects exceeding the acceptance criteria were observed on the examined surfaces or at the interlayer transition zones [40].

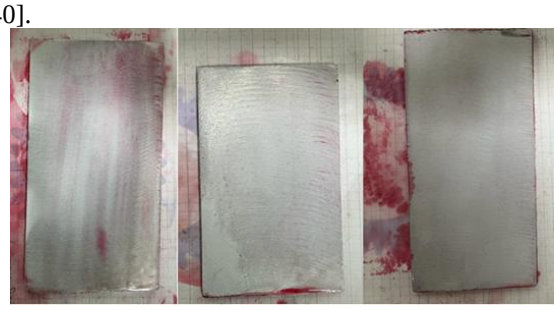

Figure 14. Specimens prepared for penetrant testing following developer application and surface cleaning [icmatse2024]

Figure 15. Specimens following the application of red penetrant during liquid penetrant testing [icmatse2024]

c. Ultrasonic test (UT)

Ultrasonic testing of the specimens following EN ISO 17640 revealed no volumetric defects, interlayer separations, or discontinuities exceeding the acceptance criteria, as illustrated in Figure 16. [41].

Köhler et al. investigated heat accumulation and the influence of varying temperature-time profiles on the properties of components fabricated via WAAM using A5356 alloy. Their findings demonstrated that heat accumulation depended on travel speed and cooling intervals, significantly influencing the resulting microstructure [36].

In a similar manner, lowering the heat input in the current study resulted in improved microstructure and a reduction in porosity within the aluminum alloy components. To accomplish this, the optimal setup should incorporate increased travel speeds and extended cooling durations to minimize pore diameter.

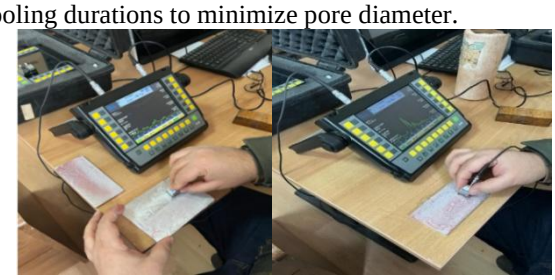

Figure 16. Specimen subjected to ultrasonic inspection [icmatse2024]

2.11. Archimedes' Principle

Archimedes' principle states that an object immersed in a fluid experiences an upward buoyant force equal in magnitude to the weight of the fluid displaced by the object. In Table 8, according to Archimedes' Principle, the differences in the porosities that will occur in the material in the samples taken parallel and perpendicular to the fabrication direction were examined. The specimens taken in the production direction were observed to have higher density in the samples with the same heat input.

As a result, reduced heat input and lower heat accumulation lead to smaller pore sizes. A slight reduction in pore diameter is also observed with increased travel speed and extended cooling time.

Minimized heat accumulation positively influences porosity characteristics [36, 42, 43].

Despite this, the second wall—aligned perpendicular to the rolling direction—exhibited favorable heat input characteristics and reduced porosity. In assessing wall densities, specimens extracted perpendicular to the rolling direction consistently displayed lower density values than those oriented parallel to the rolling direction [10, 36, 42, 43].

Table 8. Density results from Archimedes' principle. (R.D: Rolling Direction, P.R: Perpendicular Rolling) [icmatse2024]

Specimen	Air (g)	Aqua (g)	Density (g/cm^3)
1st Wall R.D.	6.26	2.39	2.6152
1st Wall P.R.	7.15	2.74	2.6016
2nd Wall R.D.	6.52	2.51	2.5993
2nd Wall P.R.	6.07	2.33	2.5954
3rd Wall R.D.	6.42	2.44	2.6268
3rd Wall P.R.	6.57	2.50	2.6200

3. CONCLUSIONS

This study investigated the mechanical and microstructural properties of WAAM-produced A5356 alloy using various testing methods. The results showed that lower heat input increased tensile strength due to finer grains. At the same time, the second wall achieved optimal flexural performance, highlighting a trade-off between heat input and mechanical behavior.

Mechanical anisotropy was observed between the build direction and the transverse direction. SEM, optical microscopy, XRD, and EDS analyses further revealed that controlling the heat input significantly affects the formation and distribution of the β-phase (Al_3Mg_2), thereby influencing the uniformity and strength of the microstructure. Mechanical characterization through bending and hardness testing demonstrated that the wall manufactured with a controlled heat input of 125.95 J/mm attained superior mechanical properties, indicating an optimal balance between structural integrity and process parameters. Overall, these results underscore the importance of heat input optimization and demonstrate the potential of WAAM as an effective method for producing A5356 components with tailored properties.

1. Under conditions of low heat input, Wall 1—fabricated using a reduced wire feed speed (WFS) parameter—demonstrated superior flexural strength and microhardness compared to Walls 2 and 3, highlighting the beneficial effects of optimized welding parameters on mechanical performance.

2. Tensile testing conducted along the production direction and transverse to it yielded strength values of 270.97 MPa and 184.53 MPa, respectively (refer to Table 6). These findings indicate a pronounced anisotropy, with specimens aligned with the production direction exhibiting significantly higher tensile strength.

3. The application of low heat input resulted in enhanced flexural strength and microhardness; however, longitudinal tensile testing revealed relatively low tensile strength. In contrast, transverse tensile tests yielded comparable strength values across all wall

specimens, suggesting uniform mechanical behavior in that orientation.
4. Microstructure analysis showed that increasing heat input leads to dissolution of β-phase (Al_3Mg_2) and grain size increase, resulting in reduced mechanical properties.
5. SEM-EDS and XRD analysis showed the distribution of Al_3Mg_2 composition in the material and indicated that the 2nd wall sample is the optimum material.
6. Non-destructive test results showed no discontinuities on the material surface or transitions between layers exceeding the acceptance criteria during visual test (VT) and penetrant test (PT).
7. Ultrasonic testing (UT) revealed no volumetric defects, delamination between layers, or discontinuities exceeding the acceptance criteria.
8. To ensure a more thorough understanding of the material behavior, future studies should incorporate comprehensive non-destructive evaluation techniques. This includes mechanical testing, microstructural analysis, structural characterization, and systematic variation of heat input parameters, enabling a multidimensional assessment of performance and integrity.
9. The overarching objective is to enhance mechanical performance through the optimization of heat input parameters, thereby achieving superior structural integrity and material properties.
10. The specimen oriented perpendicular to the rolling direction of the second wall, produced with a heat input of 125.95 J/mm, exhibited optimal porosity for accurate density determination via Archimedes' principle.

ACKNOWLEDGMENTS

This study was supported by the Scientific and Technological Research Council of Türkiye (TÜBİTAK) under the 2209-B Industry-Oriented Undergraduate Research Projects Support Program, project code 1139B412302655. The authors would like to thank the valuable support. They would also like to thank Intecro Robotics for their valuable industrial partnership.

DECLARATION OF ETHICAL STANDARDS

The author(s) of this article declares that the materials and methods used in this study do not require ethical committee permission and/or legal-special permission.

AUTHORS' CONTRIBUTIONS

Berfin GURSU: Performing and interpreting tests and analyses, and writing the article.
Sude Merve KAYIS: Performing and interpreting tests and analyses, and writing the article.
Hakan ATES: Design of the study, interpretation, and finalization of tests, analyses, and supervision of manuscript writing and editing.
Murat KAYAALP: Performing non-destructive examinations, finding and interpreting standards.
Ozge Ece KARA: Industrial consulting within the scope of the project for conducting and interpreting tests and analyses

CONFLICT OF INTEREST

There is no conflict of interest in this study.

REFERENCES

[1] Tekeli A. F. ve Seçkin B., "Tel Beslemeli Ark Eklemeli İmalat Yönteminde Soğuk Metal Transferi Teknolojisinin Kullanımı", ***Mühendis ve Makine Dergisi***, 44: 26-30, (2020).
[2] Ayan Y., "Farklı Malzeme Katmanlı Ürünlerin Tel Ark Eklemeli İmalatı", ***Karabük University Institute of Graduate Studies, Ph.D. Thesis***, 1-25, (2022).
[3] Çakır E. ve Ulutan M., "Tel Ark Katmanlı İmalat (TAKİ) Yöntemi ve Farklı Malzemelerde Mekanik Özelliklerinin İncelenmesi", ***Bilecik Şeyh Edebali University Fen Bilimleri Dergisi***, 10: 217-235, (2023).
[4] Kayacan M. Y. ve Yılmaz N., "DMLS eklemeli imalatta süreç ve maliyet modeli geliştirilmesi", ***Politeknik Dergisi***, 22(3): 763-770, (2019).
[5] Karakılınç U., Yalçın B. ve Ergene B., "Toz yataklı/beslemeli eklemeli imalatta kullanılan partiküllerin uygunluk araştırması ve partikül imalat yöntemleri", ***Politeknik Dergisi***, 22(4): 801-810, (2019).
[6] Polat Çoban N., Anaç N. ve Mert F., "Eklemeli imalat ile üretilen PLA parçaların yapıştırılmasında yapıştırma parametrelerinin mekanik dayanımına etkisinin incelenmesi", ***Politeknik Dergisi***, 26(3): 1145-1154, (2023).
[7] Raut L. P. ve Taiwade R. V., "Wire Arc Additive Manufacturing: A Comprehensive Review and Research Directions", ***Journal of Materials Engineering and Performance***, 30: 4768-4791, (2021).
[8] Saleh B., Fathi R., Tian Y. ve diğerleri, "Fundamentals and advances of wire arc additive manufacturing: materials, process parameters, potential applications, and future trends", ***Archives of Civil and Mechanical Engineering***, 23: 96, (2023).
[9] Zhang Y., Wang L. ve Liu H., "Automated Determination of Grain Features for Wire Arc Additive Manufacturing Process", ***Journal of Materials Engineering and Performance***, 32(5): 1234-1245, (2023).
[10] Köhler M., Hensel J. ve Dilger K., "Effects of Thermal Cycling on Wire and Arc Additive Manufacturing of Al-5356 Components", ***Metals***, 10: 952-963, (2020).
[11] Özsoy K. ve Duman B., "Eklemeli İmalat (3 Boyutlu Baskı) Teknolojilerinin Eğitimde Kullanılabilirliği", ***International Journal of 3D Printing Technologies and Digital Industry***, 1: 36-48, (2017).
[12] Karayel E., Bozkurt Y., Özdemir C. ve Kalender M., "Investigation of Mechanical Properties of Aluminum Alloys Produced by Wire Arc Additive Manufacturing Method", ***Marmara University Institute of Natural and Applied Sciences, Master's Thesis***, 3-67, (2022).
[13] Mercan E., Ayan Y. ve Kahraman N., "Gazaltı metal ark kaynak (GMAK) yöntemiyle birleştirilen AA5754 ve AA6013 alüminyum alaşımlarının mikro yapı ve mekanik özellikleri", ***Pamukkale University Mühendislik Bilimleri Dergisi***, 26: 82-87, (2020).
[14] Ayan D. ve Nizamettin K., "Metal Eklemeli İmalat: Tel Ark Yöntemi ve Uygulamaları", ***International Journal of***

3D Printing Technologies and Digital Industry, 2: 74-84, (2018).

[15] Özsolak O., "Eklemeli İmalat Yöntemleri ve Kullanılan Malzemeler", ***International Journal of Innovative Engineering Applications***, 3(1): 9-14, (2019).

[16] Evrensel R. ve Ertek C., "Eklemeli İmalatta Alüminyum ve Alüminyum Alaşımlarının Uygulamaları ve Topoloji Optimizasyonu", ***Journal of the Institute of Science and Technology***, 13: 2008-2025, (2023).

[17] Gierth M., Henckell P., Ali Y., Scholl J. ve Bergmann J. P., "Wire Arc Additive Manufacturing (WAAM) of Aluminum Alloy AlMg5Mn with Energy-Reduced Gas Metal Arc Welding (GMAW)", ***Materials***, 13: 2671-2693, (2020).

[18] Nagasai B. P., Malarvizhi S. ve Balasubramanian V., "Wire Arc Additive Manufacturing of 5356 Aluminum Alloy Cylindrical Component: Mechanical Properties and Microstructural Characteristics", ***Weld Fab Tech Times***, (2023).

[19] Wang J., Feng J. C. ve Wang Y. X., "Microstructure of Al–Mg dissimilar weld made by cold metal transfer MIG welding", ***Materials Science and Technology***, 24(7): 827-831, (2008).

[20] Sachin Kumar, Gurraj Singh, Vishal S. Sharma ve diğerleri, "Investigation of Process Parameters for Quality Deposition of AL5356 using Cold Metal Transfer Wire Arc Additive Manufacturing (CMT-WAAM)", ***Research Square, Preprint***, (2024).

[21] Wang J., Shen Q., Kong X. ve Chen X., "Arc Additively Manufactured 5356 Aluminum Alloy with Cable-Type Welding Wire: Microstructure and Mechanical Properties", ***Journal of Materials Engineering and Performance***, 1-7, (2021).

[22] Wang J., Zhu K., Zhang W., Zhu X. ve Lu X., "Microstructural and defect evolution during WAAM resulting in mechanical property differences for AA5356 component", ***Journal of Materials Research and Technology***, 22: 982-996, (2023).

[23] Jiangang P., Bo Y., Jinguo G., Yu R., Hongjun C., Liang Z. ve Hao L., "Influence of arc mode on the microstructure and mechanical properties of 5356 aluminum alloy fabricated by wire arc additive manufacturing", ***Journal of Materials Research and Technology***, 20: 1893-1907, (2022).

[24] Langelandsvik G., Akselsen O. M., Furu T. ve Roven H. J., "Review of Aluminum Alloy Development for Wire Arc Additive Manufacturing", ***Materials***, 14: 5370, (2021).

[25] Li S., Zhang L. J., Ning J., Wang X., Zhang G. F., Zhang J. X., Na S. J. ve Fatemeh B., "Comparative study on the microstructures and properties of wire+ arc additively manufactured 5356 aluminum alloy with argon and nitrogen as the shielding gas", ***Additive Manufacturing***, 34: 101206, (2020).

[26] Li S., Zhang L. J., Ning J., Wang X., Zhang G. F., Zhang J. X. ve Na S. J., "Microstructures and mechanical properties of Al–Zn–Mg aluminum alloy samples produced by wire+ arc additive manufacturing", ***Journal of Materials Research and Technology***, 9: 13770-13780, (2020).

[27] Koduru J. P., Kumar T. V. ve Mantrala K. M., "A review of wire and arc additive manufacturing using different property characterization, challenges and future trends", ***International Journal of System Assurance Engineering and Management***, 15: 4563-4581, (2024).

[28] Zahid M., Hai K., Khan M., Shekha A., Pervaiz S., Moneeb Ali S., Abdul-Latif O. ve Salman M., "Wire Arc Additive Manufacturing (WAAM): Reviewing Technology, Mechanical Properties, Applications and Challenges", ***ASME International Mechanical Engineering Congress and Exposition, Proceedings***, 2A: V02AT02A042, (2020).

[29] Wieczorowski M., Pereira A., Carou D., Gapinski B. ve Ramírez I., "Characterization of 5356 Aluminum Walls Produced by Wire Arc Additive Manufacturing (WAAM)", ***Materials***, 16(7): 2570, (2023).

[30] GEKA - Gedik Kaynak, "AlMg 5 [Technical data sheet]", ***www.gedikkaynak.com.tr***, (t.y.).

[31] Karimi J., Bohlen A., Kamboj N. ve diğerleri, "Automated Determination of Grain Features for Wire Arc Additive Manufacturing", ***Journal of Materials Engineering and Performance***, 32: 10402-10411, (2023).

[32] Kayadelen A., Ateş H. ve Yılmaz O., "Wire Arc Additive Manufacturing (Metal Inert Gas-Cold Metal Transfer) of ER70S-6: Experimental and Computational Analysis on Process, Microstructure, and Mechanical Property Relationships", ***Journal of Materials Engineering and Performance***, (2025).

[33] Goldstein J., Newbury D., Joy D., Lyman C., Echlin P., Lifshin E., Sawyer L. ve Michael J., "Scanning Electron Microscopy and X-Ray Microanalysis", ***Springer***, (2018).

[34] Zuo X., Lv Z., Wang Y., Chen X. ve Qi W., "Microstructural Organization and Mechanical Properties of 5356 Aluminum Alloy Wire Arc Additive Manufacturing Under Low Heat Input Conditions", ***Metals***, 15(2): 116, (2025).

[35] Li J., Wang X. ve Zhao Y., "Wire and Arc Additive Manufacturing of High-Strength Al–Zn–Mg Alloy: Microstructure and Mechanical Properties", ***Frontiers in Materials***, 7: 656429, (2020).

[36] Köhler M., Fiebig S., Hensel J. ve Dilger K., "Wire and Arc Additive Manufacturing of Aluminum Components", ***Metals***, 9(5): 608, (2019).

[37] Sharma S. K., Chandra M., Kazmi K. H. ve diğerleri, "Surface Characteristics, Microstructural, and Tribological Behavior of Wire Arc Additive Manufactured Aluminum-5356 Alloy", ***Journal of Materials Engineering and Performance***, (2024).

[38] Liu J., Chen H., Li W. ve diğerleri, "Investigation on the microstructure and mechanical properties of 5356 aluminum alloy wire in continuous casting direct rolling process", ***Journal of Materials Science***, 59: 20428-20444, (2024).

[39] Girgsdies F., "Peak Profile Fitting in XRD", ***Electron Microscopy Group, Department of Inorganic Chemistry, Fritz-Haber-Institut der MPG, Berlin***, (2015).

[40] EN ISO 23277, "Non-destructive testing of welds - Penetrant testing of welds - Acceptance Levels", ***ISO***, (2015).

[41] EN ISO 11666-1, "Non-destructive testing of welds - Ultrasonic testing - Acceptance levels", ***ISO***, (2015).

[42] Wahsh L., Azzam M., Turky M., Salem H., Hamdy F., Mansour A. ve ElShater A., "Parameter Selection for Wire Arc Additive Manufacturing (WAAM) Process", (2018).

[43] Chen F., Yang Y. H. ve Feng H., "Regional Control and Optimization of Heat Input during CMT by Wire Arc Additive Manufacturing: Modeling and Microstructure Effects", ***Materials***, 14: 1061, (2021).